

Modelling Soil Erosion in the Densu River Basin Using RUSLE and GIS Tools

G. ASHIAGBOR¹, E. K. FORKUO¹⁺, P. LAARI² AND R. AABEYIR²

Soil erosion involves detachment and transport of soil particles from top soil layers, degrading soil quality and reducing the productivity of affected lands. Soil eroded from the upland catchment causes depletion of fertile agricultural land and the resulting sediment deposited at the river networks creates river morphological change and reservoir sedimentation problems. However, land managers and policy makers are more interested in the spatial distribution of soil erosion risk than in absolute values of soil erosion loss. The aim of this paper is to model the spatial distribution of soil erosion in Densu River Basin of Ghana using RUSLE and GIS tools and to use the model to explore the relationship between erosion susceptibility, slope and land use /land cover (LULC) in the Basin. The rainfall map, digital elevation model, soil type map, and land cover map, were input data in the soil erosion model developed. This model was then categorized into four different erosion risk classes. The developed soil erosion map was then overlaid with the slope and LULC maps of the study area to explore their effects on erosion susceptibility of the soil in the Densu River Basin. The Model, predicted 88% of the basin as low erosion risk and 6% as moderate erosion risk, 3% as high erosion risk and 3% as severe risk. The high and severe erosion areas were distributed mainly within the areas of high slope gradient and also sections of the moderate forest LULC class. Also, the areas within the moderate forest LULC class found to have high erosion risk, had an intersecting high erodibility soil group.

Key words : *Soil erosion, RUSLE, GIS modelling, remote sensing, Densu river basin*

1.0 Introduction

Soil erosion involves detachment and transport of soil particles from top soil layers, degrading soil quality and reducing the productivity of affected lands¹. Problems associated with land soil erosion, movement and deposition of sediment in rivers, lakes and estuaries persist through the geologic ages around the world². Erosion in basin areas creates superficial crust of soil to be eradicated and the arable lands to be reduced³. Soil eroded from the upland catchment causes depletion of fertile agricultural land and the resulting sediment delivered to the river networks creates river morphological change and reservoir sedimentation problems⁴.

In Africa it is estimated that the decrease in productivity due to soil erosion is 2-40% with an average of 8.2% for the whole continent and also, an average of 19% of reservoir storage volumes are silted⁵. In addition, excessive sedimentation clogs stream channels and increases costs for maintaining water conveyances. Soil erosion is one of the major non-point pollution sources in many watersheds⁶. Soil erosion, sedimentation, and the subsequent conveyance of fertilizers, pesticides, and herbicides play a significant role in impairing water resources within sub watersheds and watersheds⁷.

The need to quantify the amount of erosion in a spatially distributed form has become essential at the watershed scale and in the implementation of conservation efforts¹. In many situations, land managers and policy makers are more interested in the spatial distribution of soil erosion risk than in absolute values of soil erosion loss⁸. The aim of this paper is to model the spatial distribution of soil erosion at Densu River Basin of Ghana using RUSLE (Revised Universal Soil Loss Equation) and GIS (Geographic Information Systems) tools and explore the relationship between erosion susceptibility, slope and land use /land cover (LULC).

The identification of the spatially distributed erosion sources will make possible the implementation of special conservation efforts on these source areas. By effectively predicting soil erosion, it is possible to: develop sound land-use practices as they relate to earth disturbing activities, estimate the efficiency of best management practices required to prevent excess sediment loading, and identify target areas for conservation funds or research⁹.

The Densu River Basin (DRB) serves as a source of water for the Weija Reservoir .This catchment is influenced by the man's development activities, the soil erosion and sediment transport to the lake which decrease its capacity

¹ Department of Geomatic Engineering, Kwame Nkrumah University of Science & Technology, Kumasi, Ghana.

² Department of Environment and Resource Studies, University for Development Studies, Wa Campus, Wa, Ghana.

⁺ Corresponding author : e-mail : eforkuo.soe@knust.edu.gh.com

Modelling soil erosion in the Densu river basin using RUSLE and GIS tools

and quality. The Weija Water Works draws its water from the Weija Reservoir which was constructed in 1952 by damming the Densu River at Weija. The water is treated and supplied to west Accra and some other areas of the city. The DRB covers an area of about 2564 km² and forms part of the coastal river basins of Ghana lying between latitudes 5°30' N and 6°20' N and longitudes 0° 10' W and 0° 35' W (Fig. 1).

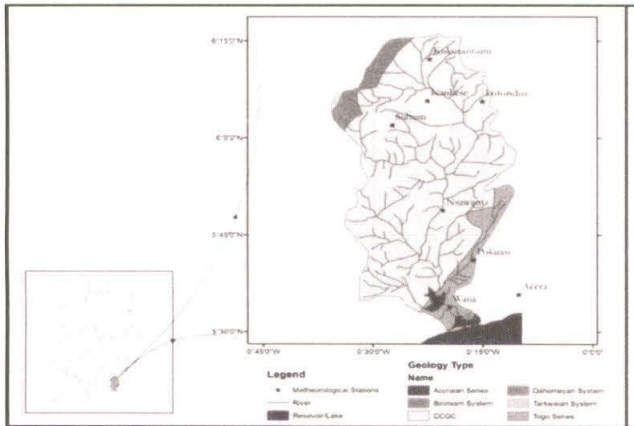


Fig. 1: Case study area: map of DRB showing major rivers in the catchment

In addition, the elevation of DRB ranges between 50 to 2750 feet above mean sea level. Effects of rapid urbanization and increasing agricultural and industrial activities in the DRB and around the reservoir have impacted the quality of water in the river and reservoir¹⁰. The DRB is of great economic importance to Ghana but not much research works have been undertaken on the basin in relation to soil erosion modelling. Runoff estimates into the Weija reservoir and their implication for water supply were modelled by Kuma and Ashley¹⁰. In their research they examined the hydrological data available on the Weija Reservoir from 1980 to 2007 in an attempt to estimate runoff into the reservoir with the view of determining whether water is available in the basin to meet the present and future demands of reservoir.

Bambury and Elgy¹¹ developed a conceptual sediment yield model for Ghana using sediment transport data based on the CALSITE model to run in the GRASS GIS package for use in Ghana. The model was tested on a 14 km² basin southwest of the Volta Lake, based on streamflow, rainfall, soil moisture and sediment transport data. GIS facilitates efficient manipulation and display of a large amount of geo-referenced data. More importantly, it allows easy definition of spatial subunits of relatively uniform properties. The use of remote sensing and (GIS) techniques makes soil erosion estimation and its spatial distribution feasible with reasonable costs and better accuracy in larger areas⁸.

Mapping soil erosion using GIS can easily identify areas that are at potential risk of extensive soil erosion and

provide information on the estimated value of soil loss at various locations⁷. Hence, with the aid of GIS, erosion and sediment yield modeling can be performed on the individual subunits. The combined use of GIS and erosion models has been shown to be an effective approach to estimating the magnitude and spatial distribution of erosion^{1, 12, 13, 14, 15}.

2.0 RUSLE parameter estimation for soil erosion modelling

This section describes the basic concepts of Revised Universal Soil Loss Equation (RUSLE) Model and methodology to estimate five parameters rainfall-runoff erosivity factor, soil erodibility, slope length factor, slope steepness factor, and land cover management factor. In addition, modelling the potential erosion susceptible areas are described.

2.1 RUSLE parameter estimation

The RUSLE is the most widely used soil loss estimation method¹⁶. The equation is the update of the original Universal Soil Loss Equation¹⁷. In RUSLE, the rainfall runoff factor of the original USLE was replaced by the rainfall erosivity factor while K , LS , C and P are the same parameters as in the original USLE factors⁴. The RUSLE computes the average annual erosion expected on field slopes and is shown in equation 1.

$$A = R * K * LS * C * P \quad \dots (1)$$

Where: A is annual soil loss from sheet and rill erosion expressed in tons per hectare per year (t/ha/yr), R is rainfall erosivity factor, K is soil erodibility factor, LS is slope length and steepness factor, C is cover and management factor, and P is support practice factor.

2.1.1 The rainfall erosivity (R)

Rainfall and runoff play an important role in the process of soil erosion and are together usually expressed as the R factor. The greater the intensity and duration of the rain storm, the higher the erosion potential¹⁸. The RUSLE rainfall-runoff erosivity factor (R) for any given period is obtained by summing for each rainstorm the product of total storm energy (E) and the maximum 30-minute intensity (I_{30}). Unfortunately, the values of these factors are rarely available at standard meteorological stations.

Fortunately, long-term average R -values are often correlated with more readily available rainfall values like annual rainfall or the modified Fournier's index¹⁹. For the computation of R factor, data from seven meteorological stations within the catchment was used and Schreiber's method²⁰ (as expressed in Equation 2) was then applied for determining the precipitation change according to the elevation.

$$Ph = Po + 4.5 * h(MJha^{-1}year^{-1}) \quad \dots (2)$$

Where Ph is the average annual precipitation (mm) and Po represents the amount of average annual rainfall (mm) at chosen meteorological station and h (measured in mega Joule per hector per year) is elevation of the place which the precipitation is be calculated. From the results of this calculation (as shown in Fig. 2), a rainfall factor layer was then generated with ESRI ArcGIS over the whole study area by using an inverse distance weighting interpolation algorithm on a 30m resolution. The resultant Digital Elevation Model (DEM) is shown in Fig. 2a while the rainfall (R-factor) distribution is shown in Fig. 2b.

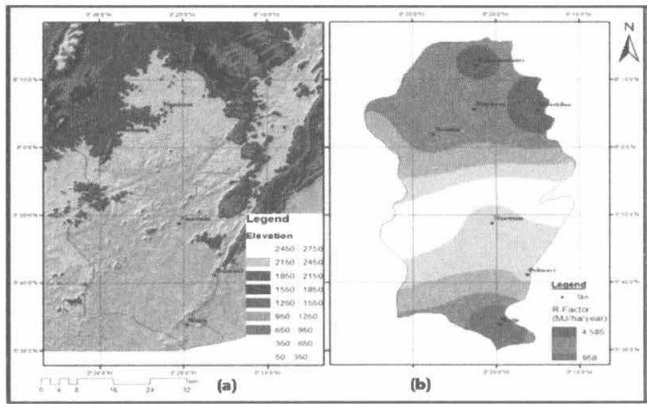


Fig. 2: DEM of study area (a) and R-factor distribution map (b)

2.1.2 The slope length and steepness factors (LS)

The Slope Length and Steepness Factors (LS) factor represents erodibility due to combinations of slope length and steepness relative to a standard unit plot. It expresses the effect of topography, specifically hill slope length and steepness, on soil erosion. An increase in hill slope length and steepness results in an increase in the LS factor²¹. The slope length factor (L) is defined as the distance from the source of runoff to the point where either deposition begins or runoff enters a well-defined channel that may be part of a drainage network.

On the other hand, the steepness factor (S) reflects the influence of slope steepness on erosion¹⁷. As already pointed out, the longer the slope length, the greater the amount of cumulative runoff, and the steeper the slope of the land the higher the velocities of the runoff which contribute to erosion. For estimation of the LS factor, theoretical relationship based on unit stream power theory has been adopted as this relation is best suited for integration with the GIS¹⁵. The relation is given in equation 3.

$$LS = \left[\frac{As}{22.13} \right]^{m1} \left[\frac{\sin \beta}{0.0896} \right]^{m2} \quad \dots (3)$$

Where As is the specific area (A/b), defined as the upslope contributing area for overland grid (A) per unit width normal to flow direction (b), β the slope gradient in degrees $n= 0.4$ and $m= 1.3$. However, with the incorporation of DEM into GIS, the slope gradient (S) and slope length (L) may be determined accurately and combined to form a single factor known as the topographic factor LS. The precision with which it can be estimated depends on the resolution of the DEM²².

Using the Spatial Analyst Extension (as implemented in ArcGIS), the slope of the catchment area was derived from DEM. Sinks in the DEM were identified and filled. The filled DEM was used as input to determine the Flow Direction which was used as an input grid to derive the Flow Accumulation. The LS factor was then computed using Raster Calculator in ArcGIS to build an expression for estimating LS, based on flow accumulation and slope steepness²³. The expression is:

$$LS = Pow \left([flow\ accumulation] * \frac{resolution}{22.104} \right) * Pow \left(\sin \frac{[slope\ of\ DEM]}{0.0914} \right) * 1.4 \quad \dots (4)$$

Where Pow (which then means power) is a function in the ArcGIS spatial Analyst.

2.1.3 The land cover management factor (C)

The Land Cover Management Factor (C) is used to express the effect of plants and soil cover²¹. Plants can reduce the runoff velocity and protect surface pores. The C-factor measures the combined effect of all interrelated cover and management variables, and it is the factor that is most readily changed by human activities²¹.

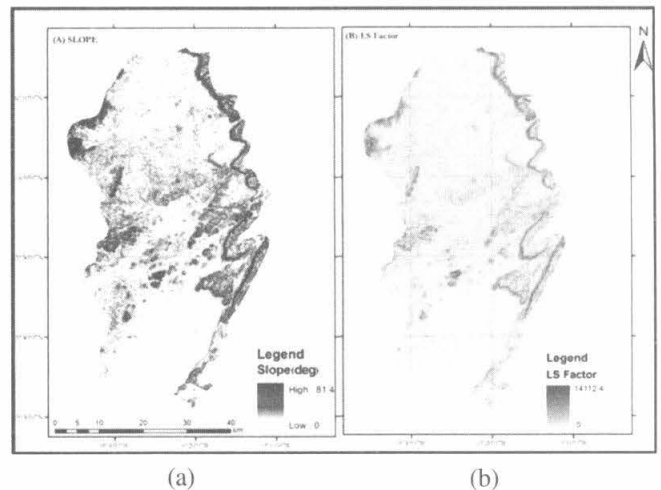


Fig. 3 : Slope map of basin (a) and LS-factor distribution (b)

Modelling soil erosion in the Densu river basin using RUSLE and GIS tools

It is mainly related to the vegetation's cover percentage and it is defined as the ratio of soil loss from specific crops to the equivalent loss from tilled, bare test-plots²⁴. The value of *C* depends on vegetation type, stage of growth and cover percentage.

The vegetation cover has a big impact in the erosion by intercepting the rainfall thus increase the infiltration and reducing the rainfall energy². *C*-factor is measured as the ratio of soil loss from land cropped under specific conditions to the corresponding loss from tilled land under continuous fallow conditions²⁵. By definition, *C* equals 1 under standard fallow conditions. As surface cover is added to the soil, the *C* factor value approaches zero. A *C* factor of 0.15 means that 15% of the amount of erosion will occur compared to continuous fallow conditions²⁶. Since the satellite image data provide up to date information on land cover, the use of satellite images in the preparation of land cover maps is widely applied in natural resource surveys²¹.

Traditionally, *C*-values are assigned to land cover classes from USLE/RUSLE guide tables or field observation. Since the Normalized Difference Vegetation Index (NDVI) values have correlation with *C* factor many researchers used regression analysis to estimate *C* factor values for land cover classes in erosion assessment²¹. These methods employ regression model to make correlation analysis between *C* factor values measured in field or obtained from guide tables and NDVI values derived from remotely sensed images. The unknown *C* factor values of land cover classes can be estimated using equation obtained from linear regression analyses.

In this research, a LandSat ETM, August 2004 with resolution 30 m was used in *C* factor calculation. The image was processed with a supervised classification to prepare the land use/cover map of the study area. In this study, an overall accuracy result of 82% was obtained from maximum likelihood classifier. Using this classifier, the DRB was classified into five LULC classes namely Dense Forest, Moderate Forest, Agricultural Land, build up and water bodies. **Fig. 4a** shows the classified image map with six classes. To estimate the *C* values NDVI was calculated from the satellite Image. 50 forest and 30 bare ground NDVI points were sampled randomly with the assumption that there exists a linear correlation between NDVI and *C* factor using forest and bare ground as reference points with forest as 1 and bare ground as 0 in the regression analysis. The regression equation was found as :

$$y = 2.48x - 0.03 \quad \dots(5)$$

Using the raster calculator in ArcGIS, a *C* Factor map (as in **Fig. 4c**) was developed for the catchment using the

correlation equation on the NDVI image map (as can be seen in **Fig. 4b**.)

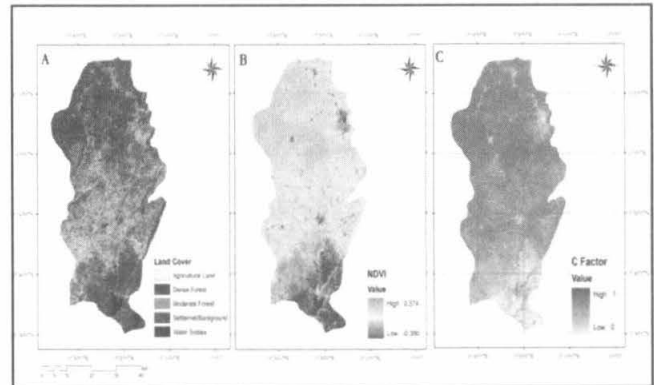


Fig. 4: Classified LULC thematic map of basin (A), NDVI (B), and C-Factor map (C)

2.1.4 Soil erodibility (K-factor)

The Soil Erodibility (*K*) factor represents both susceptibility of soil to erosion and the amount and rate of runoff. Soil texture, organic matter, structure and permeability determine the erodibility of a particular soil²⁰. The *K* factor reflects the ease with which the soil is detached by splash during rainfall and/or by surface flow, and therefore shows the change in the soil per unit of applied external force of energy²⁵. It is related to the integrated effects of rainfall, runoff, and infiltration on soil loss, accounting for the influences of soil properties on soil loss during storm events on upland areas⁸. A simpler method to predict *K* was presented by Wischmeier and Smith¹⁷ which includes the particle size of the soil, organic matter content, soil structure and profile permeability. The soil erodibility factor *K* can be approximated from a monograph if this information is known. The USLE monograph estimates erodibility as:

$$k = 2.1 * M_{1.14} * 10^{-6} * (12 - MO) + 0.0325 * (b - 2) + 0.025 * (c - 3) \quad \dots (6)$$

Where: *M* is (% Silt + % Very Fine Sand) (100- %Clay), *MO* is the percent organic matter content, *b* is soil structure code, and *c* is the soil permeability rating. For computing the *K* factor soil map available for the catchment was used. There are 8 different soils on the area (**Table 1**) based on the FAO-UNESCO soil map data classification²⁷. Not all soils have information about structure and permeability. The percentages of clay, silt, sand and organic matters were determined for each major soil type using Harmonized World Soil Database (HWSD). To obtain the *K* factor for soil the ERFAC (Proposed Alternative Soil Erodibility Factor) equation 4 was used.

Table 1: Soil erodibility factor (K) value for the different soil type

Soil Type	Clay (%)	Silt (%)	Sand (%)	ERFAC (k)
Acrisols	24	27	49	0.255
Lixisols	24	20	56	0.234
Phlinthosols	22	29	49	0.261
Leptosols	23	34	43	0.275
Fluvisols	20	41	39	0.295
Luvisols	24	20	56	0.234
Arenosols	8	10	82	0.194
Solonetz	38	60	2	0.351

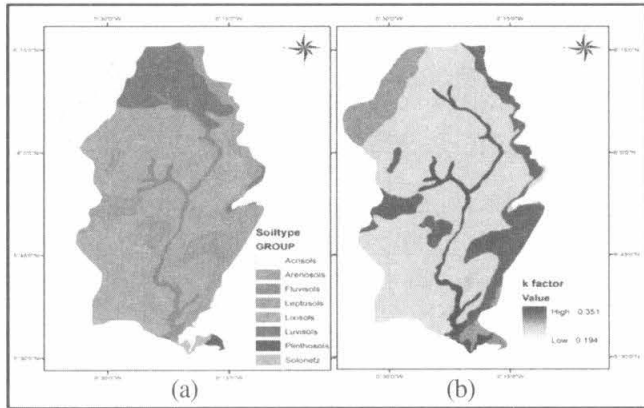


Fig. 5: Soil type map (a) and K-factor map (b)

$$ERFAC = 0.32 * \left[\frac{\% \text{ silt}}{\% \text{ sand} + \% \text{ clay}} \right]^{0.27} \dots (7)$$

With these results, the spatial distribution of the k factor was computed under a GIS (ArcGIS) at 30 meters resolution.

2.1.5 Soil conservation practice factor (P)

The soil conservation practice factor describes the supporting effects of practices like contouring, strip cropping, and terraces. Most often this variable is assigned a value 1 indicating that there are no support practices in place within the study area. Since this study focuses on the evaluation of soil erosion risk, instead of estimation of actual soil erosion loss, the P-factor value of 1 was used. So the soil erosion risk was developed based on R, K, LS, and C factors in a simplified equation.

2.2 Modelling potential erosion susceptible areas using GIS

Fig. 6 summarizes the step by step methodology of the erosion modelling process. Raster maps of the R, K, LS, and C grid layers were integrated within the ArcGIS environment using RUSLE equation 1, to generate composite maps of estimated erosion loss within the basin.

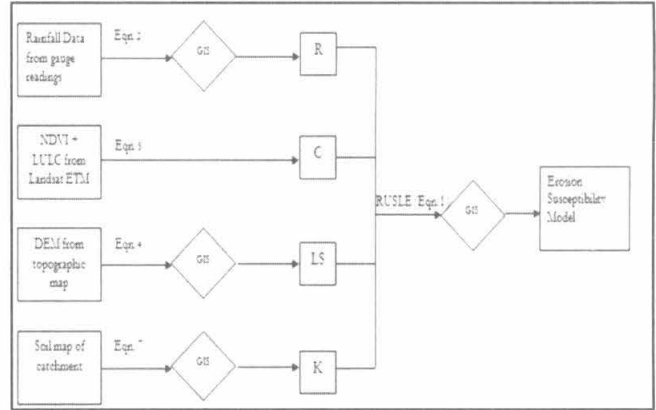


Fig. 6: Flow chart for potential soil erosion model design

The resultant map is shown in **Fig. 7** and the results are discussed in Section 3.

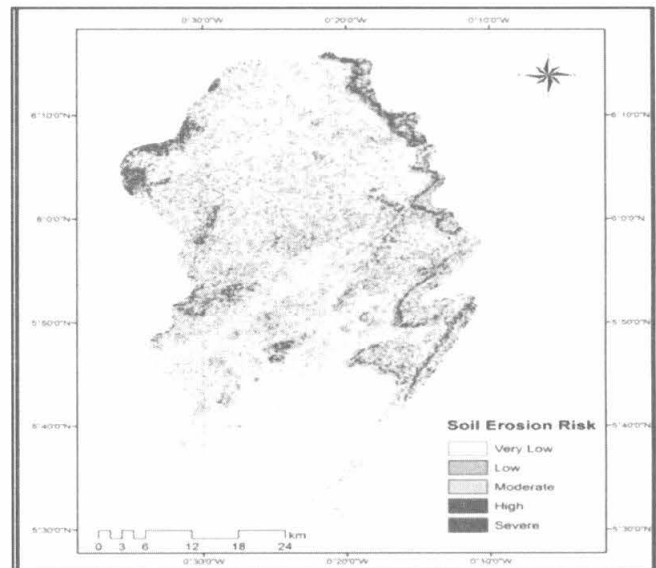


Fig. 7: Erosion risk map

The potential erosion map produced was overlaid on the slope and LULC map in the GIS environment to examine the relationship between slope and LULC on erosion in the catchment. Through the overlaying, the areas with high susceptibility in relation to slope and LULC have been identified and represented in **Fig. 8a** and **8b** respectively.

3.0 Results and discussion

The combined use of GIS and erosion models has been integrated to estimate the magnitude and spatial distribution of erosion of the study area. Five different erosion risk factors including rainfall erosivity, slope length and steepness, land cover management, soil erodibility, and soil conservation were determined. The results of modelling these factors are shown in **Fig. 2, 3, 4,** and **5**. In modelling the rainfall

Modelling soil erosion in the Densu river basin using RUSLE and GIS tools

erosivity, it can be seen that (as in Fig. 2) the greater the intensity and duration of the rain storm, the higher the erosion potential. Fig. 3 presents the results of modelling the slope length and steepness. It is noted that the longer the slope length, the greater the amount of cumulative runoff. The soil erosion susceptibility with slope categories shows that the steeper the slope of the land the higher the velocities of runoff which contribute to erosion (Fig. 8) as observed by Wischmeier and Smith¹⁷. Similarly, the land cover management factor was modelled and the results are shown in Fig. 4. The results indicate that the vegetation cover has an impact in the erosion by intercepting the rainfall thus reducing the rainfall energy and increasing the infiltration. In Fig. 5, soil erodibility factor which represents both susceptibility of soil to erosion and the amount and rate of runoff is shown. The results reflect the ease with which the soil is detached by splash during rainfall and or by surface flow, and therefore shows the change in the soil per unit of applied external force of energy.

The final soil loss model (Fig. 7) predicts that approximately in 87% of the basin has low erosion risk (i.e., erosion with very gentle runoff speed.) and 6% moderate (i.e., shallow to deep hills mainly found around agricultural lands and moderate forest class). But the erosion risk is high (i.e., very deep hills and some gullies) on 3% and severe on 3% of the catchment area. In addition to modelling the five risk factors, erosion susceptibility with respect to LULC and slope categories were modelled and are graphed in Fig. 8a and 8b. What is the most evident in the results (as can be seen in Fig. 8b) is that about 92% area of the watershed has a gradient

less than 7°, while the remaining 8% of the area has a gradient greater than 7°. This accounts to the general low susceptibility of the basin to erosion. It is also noted that the steep slopes have much higher rate of erosion compared with flat areas. Generally, it can be seen that the average rate of soil loss and the contribution to the total soil loss from steeper slope is tremendously higher compared with that of gentle slope.

The results indicate that (as in Fig. 8a) erosion risk was generally low across all the LULC classes. However, traces of severe erosion are available in the moderate forest class. From visual interpretation of the various factors, this was found to be due to the high erodibility of the soil group (leptosols) that intersects the sections of the moderate forest LULC Class. Also the moderate forest class falls within the high rainfall zones of the study area which may contribute to high erosion within the moderate forest cover class.

4.0 Conclusions and recommendations

In this paper, a soil erosion model at Densu River Basin with the integration of RUSLE and GIS tools has been developed to estimate the annual soil loss. Different components of RUSLE were modelled using various mathematical formulae to explore the relationship between erosion susceptibility, slope and LULC maps. The erosion map produced was then categorized into five different erosion risk classes. According to this model, approximately in 88% of the basin has low erosion risk and 6% moderate erosion risk. But erosion risk is high on 3% and severe on 3% of the basin.

The high and severe erosions were found to be distributed mainly within the areas of high slope gradient and also sections of the moderate forest LULC class. The results indicated that areas within the moderate forest LULC class have a high erosion risk and this was due to the presence of an intersecting high erodibility soil group. However, since the vegetative cover is a major factor of soil erosion, in future research, an NDVI should be derived from up to date and higher resolution satellite imagery. This will improve the accuracy of the LULC maps and DEMs generated for land slopes calculations. Also, an additional study is needed to determine the appropriate P-factor values within the study area to realistically estimate the potential soil erosion. In general, it is clear from the results of this study that the developed model is beneficial for the rapid assessment of soil erosion.

References

1. Fernandez, C., Wu, J., McCool, D., and Stockle, C., Estimating Water Erosion and Sediment Yield with GIS, RUSLE, and SEDD. *Journal of Soil and Water Conservation*, 58 (3), 128-136 (2003).

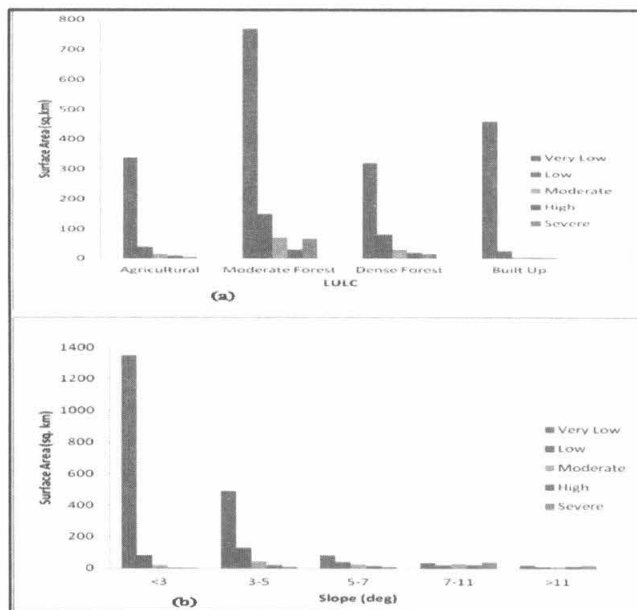


Fig. 8: Erosion susceptibility with respect to LULC (a) and slope categories (b)

2. Rojas-González, A. M., Soil Erosion Calculation Using Remote Sensing and GIS in Río Grande de Arecibo Watershed, Puerto Rico. *Proceedings ASPRS 2008 Annual Conference Bridging the Horizons: New Frontiers in Geospatial Collaboration*, Portland, Oregon, April 28th–May 2nd, p6 (2008).
3. Gandomkar, A., Shaikhe, N., Ahmadi, S., The Valuation of Erosion at Basin Watershed in Mousabad - Tiran by using SlemsaModle. *Journal of Geographical Landscape*, 3(6), 95-108 (2008).
4. Geleta, H. I., Watershed Sediment Yield Modelling for Data Scarce Areas. PhD Dissertation, University of Stuttgart (2011). . Available at <http://elib.uni-stuttgart.de/opus/volltexte/2011/6152/>. Date Accessed: 10 February, 2011.
5. Andersson, L., *Soil Loss Estimation Based on the USLE/ GIS Approach through Small Catchments - A Minor Field Study in Tunisia*. PhD Dissertation, Division of Water Resources Engineering, Department of Building and Environmental Technology, Lund University, Sweden (2010).
6. Wang, X., and Cui, P., Support Soil Conservation Practices by Identifying Critical Erosion Areas within an American Watershed Using the GIS-AGNPS Model. *Journal of Spatial Hydrology*, 5(2), 31- 44 (2005).
7. Todd, B., Assessment of Soil Erosion Risk within a Sub watershed Using GIS and RUSLE with a Comparative Analysis of the Use of STATSGO and SSURGO Soil Databases. *Resource Analysis*, 8, 1-22 (2006).
8. Lu, D., Li, G., Valladares, G. S. and Batistella, M., Mapping Soil Erosion Risk in Rondonia, Brazilian Amazonia: Using RUSLE, Remote Sensing and GIS. *Land Degradation and Development*, 499–512 (2004).
9. Hickey, R., Burns, E., Bolte, J. and Walker, D., Development of a Statewide Erosion Vulnerability Screening Tool for Oregon (2005). Available at <http://www.siue.edu/geography/online/hickey05.pdf>. Date Accessed: July 14, 2011.
10. Kuma, J. S. and Ashley, D. N., Runoff Estimates into the Weija Reservoir and Its Implications for Water Supply to Accra, Ghana. *Journal of Urban and Environmental Engineering*, 2(2), 33-40 (2008).
11. Bambury, M. and Elgy, J., Development of a Sediment Yield Model for Ghana Using Sediment Transport Data, Proceedings of the Oslo Workshop on Erosion and Sediment Transport Measurement in Rivers: Technological and Methodological Advances, *IAHS*. p 96-102 (2002).
12. Kothiyari, U. C. and Jain, S. K., Sediment Yield Estimation Using GIS. *Hydrological Science Journal*, 42 (6), 833-843 (1997).
13. Nasir, A., Uchida, K. and Ashraf, M., Estimation of Soil Erosion by Using RUSLE and GIS for Small Mountainous Watersheds in Pakistan. *Pakistan Journal of Water Resources*, 10(1), 11-21 (2006).
14. Amiri, F. and Tabatabaie, T., EPM Approach for Erosion Modeling by Using RS and GIS, *FIG Regional Conference on Spatial Data Serving People: Land Governance and the Environment – Building the Capacity* Hanoi, Vietnam, 19-22 October, p10 (2009).
15. Jain, M. K., Mishra, S. K. and Shah, R. B., Estimation of Sediment Yield and Areas Vulnerable to Soil Erosion and Deposition in a Himalayan Watershed Using GIS. *Current Science*, 98 (2), 213-221 (2010).
16. Renard, K. G., Foster, G. R., Weesies, G. A., McCool, D. K. and Yoder, D. C., Predicting of Soil Erosion by Water: A Guide to Conservation Planning with the Revised Universal Soil Equation (RULSE). Agricultural Handbook 703. Washington, DC: US. Department of Agriculture (1997).
17. Wischmeier. W. H. and Smith, D. D., Predicting Rainfall Erosion Losses: A Guide to Conservation Planning, *Agriculture Handbook 537*. Washington, D.C: US, Department of Agriculture, p58 (1978).
18. Stone, R.P. and Hilborn, D., Universal Soil Loss Equation (USLE), Agricultural and Rural Ministry of Agriculture, Food and Rural Affairs, Ontario, Canada (2000). Available at <http://www.gov.on.ca/OMAFRA/english/engineer/facts/00-001.htm>. Date Accessed: 5th Februart, 2011.
19. Sadeghi S. H. R., Moatamednia, M. and Behzadfar, M., Spatial and Temporal Variations in the Rainfall Erosivity Factor in Iran: *Journal of Agricultural Science Technology*. 13, 451-464 (2011).
20. Efe, R., Ekinci, D. and Curebal, I., Erosion Analysis of Sahin Creek Watershed (NW of Turkey) Using GIS Based on RUSLE (3d) Method. *Journal of Applied Science*, 8 (1), 49-58 (2008).
21. Karaburun, A., Estimation of C Factor for Soil Erosion Modeling Using NDVI in Buyukcekmece Watershed. *Ozean Journal of Applied Sciences* 3(1), 77-85 (2010).
22. Simms, A. D., Woodroffe, C. D. and Jones, B. G., Application of RUSLE for Erosion Management in a Coastal Catchment, Southern NSW, *Proceedings of MODSIM*

Modelling soil erosion in the Densu river basin using RUSLE and GIS tools

- 2003, *International Congress on Modelling and Simulation*, volume 2, pp 678-683 (2003)./
23. Mitasova, H., Hofierka, J., Zlocha, M., and Iverson, R., Modelling Topographic Potential for Erosion and Deposition using GIS. *International Journal of Geographical Information Systems*, 10(5), 629-641 (1996).
 24. Gitas, I. Z., Douros, K., Minakou, C., Silleos, G. N. and Karydas, C. G., Multi-Temporal Soil Erosion Risk Assessment. In N. Chalkidiki using a Modified USLE Raster Model. *Earsel Eproceedings* 8, p.40-52 (2009).
 25. Dumas, P. and Printemps, J., Assessment of Soil Erosion Using USLE Model and GIS for Integrated Watershed and Coastal Zone Management in the South Pacific Islands. *Proceedings, International Symposium in Pacific Rim*, p 856-866 (2010).
 26. Kelsey K. and Johnson T., Determining Cover Management Values (C factors) for Surface Cover Best Management Practices (BMPs). *Proceedings of the International Erosion Control Association's 34th Conference*, p 319-328 (2003).
 27. FAO-UNESCO., FAO-UNESCO (Food and Agriculture Organization and United Nations Educational, Scientific and Cultural Organization) Soil Map of the World, 1:5,000,000, Volume VI, UNESCO, Paris (1987).
-